JPP JOURNAL OF Pharmacy and Pharmacology
ROYAL PHARMACEUTICAL SOCIETY
JPP Journal of Pharmacy And Pharmacology
Research Paper

Pharmacological characterization of high-affinity σ_1 receptor ligands with spirocyclic thienopyran and thienofuran scaffold

Dirk Schepmann[a], Christina Neue[a], Stefanie Westphälinger[a], Christoph Müller[b], Franz Bracher[b], Carsten Lange[c], Patrick Bednarski[c], Carmen Almansa[d], Kristina Friedland[e], Vivien Räbiger[a], Martina Düfer[a] and Bernhard Wünsch[a,f]

[a]Institut für Pharmazeutische und Medizinische Chemie der Westfälischen Wilhelms-Universität Münster, [b]Department of Pharmacy – Center for Drug Research, Ludwig-Maximilians University of Munich, Munich, [c]Department of Pharmaceutical and Medicinal Chemistry, Institute of Pharmacy, University of Greifswald, Greifswald, Germany, [d]Esteve Pharmaceuticals S.A., Barcelona, Spain, [e]Pharmacology and Toxicology, Pharmacy and Biochemistry, Johannes Gutenberg University, Mainz and [f]Cells-in-Motion Cluster of Excellence (EXC 1003 – CiM), Westfälische Wilhelms-Universität Münster, Münster, Germany

Keywords
antiallodynic activity; calcium influx; inhibition of tumour cell proliferation; spirocyclic piperidines; σ_1 receptor ligands

Correspondence
Bernhard Wünsch, Institut für Pharmazeutische und Medizinische Chemie der Westfälischen Wilhelms-Universität Münster, Corrensstraße 48, D-48149 Münster, Germany.
E-mail: wuensch@uni-muenster.de

Received August 2, 2019
Accepted October 21, 2019

doi: 10.1111/jphp.13196

Abstract

Objectives In this study, the pharmacological properties of six spirocyclic piperidines **1**–**6** showing very high σ_1 receptor affinity (K_i = 0.2–16 nM) were investigated.

Methods *In vitro* receptor binding studies, retinal ganglion assay and *in vivo* capsaicin assay were used to determine the affinity, selectivity and activity. Influence on human tumour cell growth (cell lines A427, LCLC-103H, 5637 and DAN-G) was determined in different assays. The effect on the ergosterol and cholesterol biosynthesis was determined by GLC/MS analysis.

Key findings Receptor binding studies demonstrated high selectivity for the σ_1 receptor. The increased Ca^{2+} influx mediated by **2** and the analgesic activity of **1**, **4**, **5** and **6** confirm σ_1 receptor antagonistic activity. Inhibition of human tumour cell growth further supports the σ_1 antagonistic effects. Treatment of A427 tumour cells with **2** led to cell detachment and cell degradation. Whereas the ergosterol biosynthesis was not affected, the sterol C14-reductase, a key enzyme in the cholesterol biosynthesis, was weakly inhibited.

Conclusions Due to the high selectivity, off-target effects are not expected. The antiallodynic activity underlines the clinical potential of the spirocyclic piperidines for the treatment of neuropathic pain. Due to the antiproliferative activity, the spirocyclic σ_1 antagonists represent promising antitumour agents.

Introduction

Initially, σ receptors were assigned to the class of opioid receptors due to the high affinity for (+)-benzomorphans (such as (+)-pentazocine and (+)-SKF10,047).[1] However, this classification was dismissed later on since the opioid receptor antagonists naltrexone and naloxone were not able to compensate the (+)-benzomorphan mediated effects.[2,3] Two σ receptor subtypes were pharmacologically identified and subsequently termed as σ_1 and σ_2 receptor.[4] The σ_1 receptor shows a widespread distribution within the central nervous system (CNS) as well as in peripheral tissues such as kidney, liver, lung and heart.[5–8] The corresponding σ_1 gene was cloned from several animal species and humans displaying a 95% similarity of the amino acid sequence. The human σ_1 gene encodes for a protein with 223 amino acids with a mass of approximately 23.5 kDa.[9]

The σ_1 receptor is a unique protein without any homology to other known mammalian receptors or proteins. Although the σ_1 receptor does not have any enzymatic sterol isomerase activity, the amino acid sequence shows a 30% homology to the fungal sterol $\Delta^{8/7}$-isomerase, an enzyme which catalyses a key step in the biosynthesis of ergosterol.[10,11]

© 2019 The Authors. *Journal of Pharmacy and Pharmacology* published by John Wiley & Sons Ltd on behalf Royal Pharmaceutical Society, **72** (2020), pp. 236–248
This is an open access article under the terms of the Creative Commons Attribution License, which permits use, distribution and reproduction in any medium, provided the original work is properly cited.

In 2002, Aydar *et al.*[12] postulated a σ_1 receptor model with two transmembrane domains and both C- and N-terminus located intracellularly. Very recently, the crystal structure of the σ_1 receptor together with various ligands was published.[13,14] The σ_2 receptor has not been cloned yet and is even less explored than the σ_1 receptor. Its molecular weight was estimated to be approximately 21.5 kDa.[15] Endogenous ligands for both σ receptor subtypes have not been identified yet. Neuro(active)steroids such as pregnenolone and its sulfate, progesterone, dehydroepiandrosterone (DHEA) and the hallucinogenic *N,N*-dimethyltryptamine (DMT) are discussed as potential endogenous σ ligands since they show moderate affinity towards σ_1 receptors.[16–18]

Ligands interacting with σ_1 receptors are of particular interest due to their potential for the treatment of acute and chronic neurological disorders (e.g. epilepsy, schizophrenia, depression, Alzheimer's disease, Parkinson's disease), pain especially neuropathic pain besides alleviating the symptoms of alcohol and cocaine withdrawal.[7,19–22] Also, a variety of human tumour cells expresses σ_1 and/or σ_2 receptors in high density.[23] Labelled selective σ_1 ligands might therefore be applicable for tumour imaging. As σ_1 receptors are suggested to be involved in tumour proliferation, specific ligands may represent an interesting option for cancer therapy.[24]

In 2010, Meunier and Hayashi[25] demonstrated that the knockdown of σ_1 receptors in Chinese hamster ovarian cells (CHO) resulted in a potentiation of H_2O_2-induced apoptosis. For diabetes, it has also been reported that the disease is associated with oxidative stress. In addition, an imbalance in the endoplasmic reticulum (ER) of pancreatic β-cells was described.[26–28] The imbalance leads to an accumulation of misfolded and unfolded proteins in the ER lumen, often referred to as ER stress.

Since the σ_1 receptor is considered to be an ER chaperone protein[29] and is involved in signalling between ER and mitochondria of cells, a linkage between the σ_1 receptor and oxidative stress in pancreatic β-cells might exist.

Different methods are described to discriminate between σ_1 receptor agonists and antagonists. It was shown that the σ_1 receptor is involved in the regulation of intracellular Ca^{2+} homoeostasis in retinal ganglion cells by influencing the activity of L-type voltage-regulated Ca^{2+} channels.[30] σ_1 agonists like (+)SKF-10,047 (alazocine) and opipramol inhibit the voltage-induced Ca^{2+} influx, while antagonists (e.g. BD1047) are able to reverse this effect.

In the capsaicin assay, σ_1 receptor antagonists inhibit mechanical hypersensitivity in mice induced by injection of capsaicin in the hind paw. The antiallodynic effect of σ_1 antagonists is reversed by σ_1 agonists.[31,32] With PC12 cells, which represent an *in vitro* model of neuronal differentiation,[33] it could be demonstrated that stimulation with σ_1 receptor agonists potentiates neurite outgrowth and elongation induced by growth factors, such as nerve growth factor (NGF) or epidermal growth factor (EGF).[34]

A large number of structurally diverse molecules interact with σ_1 receptors. With the aim to find selective and potent σ_1 receptor ligands and to gain insight into possible interactions within the binding site, a broad collection of substituted spirocyclic compounds with an annulated thiophene ring was synthesized in our laboratory and the σ_1 affinity was evaluated.[35–38] Particular high σ_1 affinity was found for the spirocyclic piperidines **1**–**6** displayed in Figure 1. While in many published articles the affinity of σ ligands towards σ and related receptors, such as the PCP binding site of the NMDA receptors, was studied, an in depth investigation of affinity of **1**–**6** to other targets and the activity in different functional assays to discriminate between agonistic and antagonistic activity or elucidate the therapeutic potential has not been performed.

Usually, particular features associated with the σ_1 receptor were investigated with a particular compound or class. Herein, various pharmacological aspects of σ_1 receptors were investigated with a coherent set of potent spirocyclic σ_1 ligands **1**–**6** for the first time. First, the selectivity of the compounds was investigated in a variety of different binding assays, including opioid receptors, 5-HT receptors, serotonin transporter protein (SERT) and two different binding sites of the NMDA receptor. After determination of binding affinity, the ligands were studied in different cell-based assays as well as in an animal model of pain.

With the aim to classify the σ ligands as agonists or antagonists, the functional activity was studied in the *in vitro* retinal ganglion cell assay and in the *in vivo* capsaicin assay.

Since σ_1 receptors are also expressed on various tumour cell lines, the effect of the σ_1 receptor ligands on the proliferation of A427 (non-small cell lung cancer), LCLC-103H (large cell lung cancer), 5637 (bladder cancer) and DAN-G (pancreatic cancer) tumour cell lines was studied.

Stimulated by the structural similarity between the σ_1 receptor and fungal sterol $\Delta^{8/7}$-isomerase, the effects of the ligands on the biosynthesis of ergosterol in fungi and cholesterol in human cells were investigated.

Finally, the possible connection between the σ_1 receptor and ER mediated oxidative stress prompted us to study the influence of one of our σ_1 receptor ligands on the rate of apoptosis of murine pancreatic β-cells. If the σ_1 receptor ligand is able to modulate the cell death rate of β-cells, the σ_1 receptor could emerge as a new target in diabetes research.

The broad pharmacological evaluation of a coherent set of potent σ_1 receptor ligands considering so many different aspects, including receptor affinity, selectivity, influence on ion channels, ergosterol and cholesterol biosynthesis, ER

© 2019 The Authors. *Journal of Pharmacy and Pharmacology* published by John Wiley & Sons Ltd on behalf Royal Pharmaceutical Society,

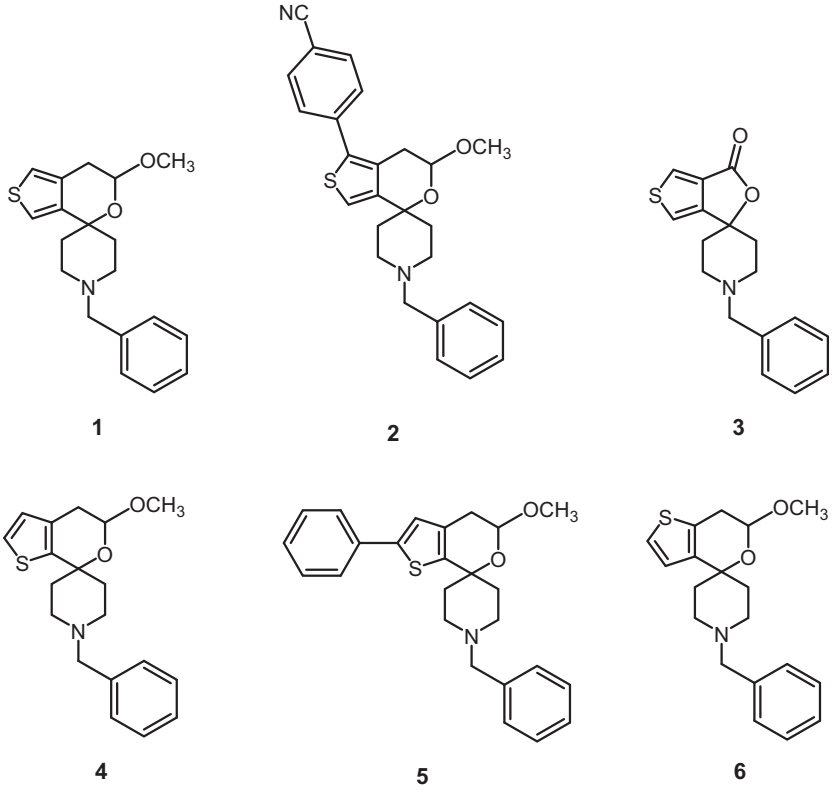

Figure 1 Spirocyclic piperidines **1**–**6** with high σ_1 receptor affinity.

stress in mouse pancreatic β-cells, tumour cell growth and proliferation, and, finally, analgesic activity *in vivo*, represents the unique feature of this study. Moreover, the aspect of σ_1 antagonistic activity was approached from various sides for the first time.

Materials and Methods

Receptor binding studies

(**1**) Details on the assay to determine the affinity towards the ifenprodil binding site of GluN2B subunit containing NMDA receptors are given in Ref. [39].
(**2**) PCP binding assay see Refs [40,41].
(**3**) σ_1 and σ_2 receptor assay see Refs [42,43].
(**4**) Affinity towards the opioid receptors KOR, DOR and MOR see Appendix S1 Refs [45,46].

Affinity towards 5-HT$_{1A}$, α_1, and α_2 receptors and 5-HT transporter

Performance of the binding assay for the human 5-HT$_{1A}$ receptor

Human 5-HT$_{1A}$ receptor enriched membranes (10 μg) were incubated with 2 nM radiolabelled [^{3}H]-8-hydroxy-DPAT in 250 μl of assay buffer containing 50 mM Tris-HCl, 5 mM $MgCl_2$, pH 7.4. NSB (non-specific binding) was measured by adding 10 μM 5-HT in 25 μl volume. Final DMSO concentration was 0.1% (v/v). After 2 h incubation at 37 °C, binding reaction was terminated by filtering 200 μl through Multiscreen GF/C (Millipore, Merck, Darmstadt, Germany) presoaked in 150 μl of 0.5% polyethylenimine in Vacuum Manifold Station, followed by three washes with 200 μl/well of ice-cold filtration buffer containing 50 mM Tris-HCl, pH 7.4.

Performance of the binding assay for the human α_{1A} adrenoreceptor

Human α_{1A} adrenoreceptor enriched membranes (10 μg) were incubated with 0.2 nM of radiolabelled [^{3}H]-prazosin in 250 μl of assay buffer containing 50 mM HEPES, 5 mM $MgCl_2$, 1 mM $CaCl_2$, 0.2% BSA, pH 7.4. NSB (non-specific binding) was measured by adding 1 μM prazosin in 25 μl volume. Final DMSO concentration was 0.1% (v/v). After 90 min incubation at 25 °C, binding reaction was terminated by filtering 200 μl through Multiscreen GF/C (Millipore) presoaked in 150 μl of 0.5% polyethylenimine in Vacuum Manifold Station, followed by three washes with 200 μl/well of ice-cold filtration buffer containing 50 mM HEPES, 500 mM NaCl, BSA 0.1%, pH 7.4.

© 2019 The Authors. *Journal of Pharmacy and Pharmacology* published by John Wiley & Sons Ltd on behalf Royal Pharmaceutical Society, **72** (2020), pp. 236–248

Performance of the binding assay for the human α_{2A} adrenoreceptor

Human α_{2A} adrenoreceptor enriched membranes (5 μg) were incubated with 0.5 nM of radiolabelled [^{3}H]MK912 in 250 μl of assay buffer containing 25 mM sodium phosphate, pH 7.4. NSB (non-specific binding) was measured by adding 10 μM rauwolascine in 25 μl volume. Final DMSO concentration was 0.1% (v/v). After 30 min incubation at 25 °C, binding reaction was terminated by filtering 200 μl through Multiscreen GF/C (Millipore) presoaked in 150 μl of 0.5% polyethylenimine in Vacuum Manifold Station, followed by three washes with 200 μl/well of ice-cold filtration buffer containing 25 mM sodium phosphate, pH 7.4.

Performance of the binding assay for the human serotonin transporter

Human serotonin transporter (SERT) enriched membranes (3.5 μg) were incubated with 3 nM of radiolabelled [^{3}H]-imipramine in 250 μl of assay buffer containing 50 mM Tris-HCl, 120 mM NaCl, 5 mM KCl, pH 7.4. NSB (non-specific binding) was measured by adding 200 μM imipramine in 25 μl volume. Final DMSO concentration was 0.1% (v/v). After 30 min incubation at 27 °C, binding reaction was terminated by filtering 200 μl through Multiscreen GF/C (Millipore) presoaked in 150 μl of 0.5% polyethylenimine in Vacuum Manifold Station, followed by three washes with 200 μl/well of ice-cold filtration buffer containing 50 mM Tris-HCl, 0.9% NaCl (m/v), pH 7.4.

Inhibition of ergosterol and cholesterol biosynthesis

These assays were performed following the methods described by us previously Appendix S1.[11,48–51]

Ca^{2+} influx assay, fluorescence measurements with fura-2-AM

Concentrations c(Ca_i^{2+}) were measured in single PC12 cells using the fluorescent indicator fura-2-AM in combination with a monochromator-based imaging system (FEI today Thermo Fisher Scientific, Langenselbold, Germany, SCR_008452) attached to a fluid immersion objective. Cells were loaded with 0.5 μM fura-2-AM and 0.01% Pluronic F-127 for 30 min at 37 °C in a standard solution composed of 138 mM NaCl, 6 mM KCl, 1 mM $MgCl_2$, 2 mM $CaCl_2$, 5.5 mM glucose and 10 mM HEPES (adjusted to pH 7.4 with NaOH at 37 °C). Cover slips were then washed in fresh buffer for 30 min and mounted in a perfusion chamber on the stage of the microscope (Olympus EX51WI, Hamburg, Germany). For measurements of c(Ca_i^{2+}), cells were excited at 340 and 380 nm and emission was measured at 510 nm. After correction for background fluorescence, the fluorescence ratio F340/F380 of the emission was calculated. Fura-2-signals were calibrated according to the method of Grynkiewicz *et al.*,[52] using a K_D value of 224 nM. 10–20 cells were measured on slide and at least two replicates/independent experiment were conducted. At least five independent experiments were measured.

Pain behavioural studies

To evaluate the effect of drugs on mechanical allodynia induced by capsaicin, a previously described experimental procedure was used Appendix S1.[31]

Animal care, husbandry and research were conducted in a sound-attenuated, air-regulated, experimental room of the Animal Facility of the Parc Científic de Barcelona (PCB), in accordance with institutional protocols approved by the local Committee of Animal Use and Care of our Institution (Animal Research Ethics Committee) and by Generalitat de Catalunya (Registry number: 9015-368574/2016) and international standards, including the Care and Use of Laboratory Animals Guidelines of the European Community (European Directive 2010/63/EU).

ER stress

Pancreatic islets were isolated from C57BL/6N mice by collagenase digestion. Single islet cells were cultured in RPMI 1614 medium with 10% fetal calf serum and 1% penicillin/streptomycin (in 10 mM glucose). ER stress was induced by addition of 10 μM cyclopiazonic acid (CPA) for 24 h. Apoptosis was determined by TUNEL staining (*in situ* cell death detection kit, fluorescein, Roche Diagnostics, Mannheim, Germany) according to the manufacturer's protocol. For determination of the total cell number, nuclei were stained with bisbenzimide (Hoechst-33258). Fluorescence of apoptotic cells was excited at 480 nm. Nuclear staining was excited at 380 nm. A minimum of 200 cells for each condition was analysed per preparation to determine the rate of apoptosis.

Inhibition of human tumour cell proliferation

The cytotoxic effects of the test compounds were investigated in four cell lines as previously described Appendix S1.[53]

Effects on human tumour cell line A427

Cell biological experiments with A427 cells

Materials. The A427 cells were kindly provided by Prof. Dr. Joachim Jose (Münster, Germany). Medium: RPMI 1640

© 2019 The Authors. *Journal of Pharmacy and Pharmacology* published by John Wiley & Sons Ltd on behalf Royal Pharmaceutical Society,

w/ L-glutamine sterile filtered and phenol red indicator (Biowest, Nuaillé, France), FBS Superior (Biochrom AG, Berlin, Germany), penicillin/streptomycin (10 000 µg/ml) (Biochrom GmbH, Berlin, Germany). PBS Dulbecco w/o Ca^{2+}, w/o Mg^{2+}, low endotoxin and trypsin 0.25% (w/v) in PBS w/o Ca^{2+}, w/o Mg^{2+} (both Biochrom GmbH). Bovine serum albumin (VWR International GmbH, Darmstadt, Germany). Triton X 100 (Carl Roth GmbH & Co. KG, Karlsruhe, Germany).

Biological safety cabinet: Thermo Scientific™ Safe 2020. Incubator: Heracell 150i CO_2 Incubator (both Thermo Fisher Scientific). Autoclave: Systec DX-65 (Systec GmbH, Linden, Germany). Water bath: Julabo ED heating circulator with open bath (Julabo GmbH, Seelbach, Germany). Centrifuge: Centrifuge 5804 R (Eppendorf, Hamburg, Germany). Vortexer: VTX-3000L (LMS Co., Ltd., Tokyo, Japan). Cell counting: Scepter™ cell counter and Scepter™ 40 µm sensor (Merck KGaA, Darmstadt, Germany). Live Cell Imager: IncuCyte® S3 (Essen BioScience Ltd., Hertfordshire, UK). Plate reader: Mithras LB 940 (Berthold Technologies, Bad Wildbad, Germany).

Cultivation of A427 cells. For the preparation of the medium for the A427 cells 450 ml of RPMI 1640, 50 ml of FBS Superior and 5 ml of penicillin/streptomycin (10 000 µg/ml) were warmed to 37 °C in the water bath and mixed under sterile conditions in the biological safety cabinet. The content of one 2.0 ml cryovial (approx. 1–2 million cells) was added to 12 ml of the prepared medium in a 75 ml culture flask (VWR® Tissue Culture Flasks, VWR, Langenselbold, Germany). This flask was then stored in the incubator at 37 °C and a water saturated atmosphere with 5% CO_2. The unused medium was stored at 5 °C. The medium in the flask was changed when the indicator changed its colour.

Subcultivation of A427 cells. At a confluence of 80–90%, the A427 cells of one flask were split over three flasks (VWR). The medium, PBS Dulbecco and trypsin were warmed to 37 °C in the water bath. The medium was removed from the flask, and the cells were rinsed with 12 ml of PBS. After the removal of the PBS, 4 ml of trypsin were added. The cells were incubated in the incubator at 37 °C for 5–10 min until approx. 80% of the cells were detached from the surface. Then, 15 ml of medium was added. The mixture was centrifuged at 800 × *g* for 10 min at 4 °C. The supernatant was discarded, and the pellet was resuspended in 12 ml of medium by manual vortexing. The medium with the cells was equally distributed over three culture flasks (VWR) and filled up with medium to a total volume of 12 ml. The cultivation conditions were the same as described above.

Live cell imaging using the IncuCyte® S3 live cell analysis system

General remarks. The measurement of the cell confluence and the determination of the IC_{50} values were performed with the IncuCyte® S3 Live Cell Analysis System.

Preparation of 96-well plates. For the preparation of the 96-well plates for the Live Cell Imager, A427 cells from the flask were detached and centrifuged. The pellet was resuspended in 20 ml of the medium using the vortexer. 1 ml was used to determine the number of cells, and the volume required for 8000–12 000 cells was calculated. This volume was then added to each well of a sterile 96-well plate (Tissue Culture Testplates 96F 92696, TPP, Trasadingen, Switzerland), and the well was filled up to a total volume of 150 µl with medium.

At a confluence of 30–40%, the test compounds were added. Dilutions of concentrations of 200, 100, 40, 20, 10 and 4 µM were prepared in medium with 2% DMSO. 50 µl of each dilution was added to the wells, resulting in a final assay concentration of 50, 25, 10, 5, 2.5 and 1 µM, respectively. Each concentration was measured in triplicates on each plate and on three different days.

Competitive confluence assay. The plates were prepared as described above with the exception that the cells were grown in 100 µl instead of 150 µl of medium. After the cell confluence reached 30–40%, the cells were treated with the respective test compounds and the agonist (+)-pentazocine (final concentration: 10 µM).

Measurement of cell confluence. The cell confluence was measured using the IncuCyte® S3. For the scanning with the company's own programme (IncuCyte S3 2017A), the HD phase imaging mode was chosen at a 10-fold magnification. Four pictures were taken from each well every 2 h until the growth curve of the cells reached a plateau (approx. 5 days). The mask for the analysis of the confluence in the pictures had a segmentation adjustment of 1.1, a cleanup adjustment size of −1 pixel and an area filter of minimum 200 μm^2. After the analysis, a graph showing the development of the confluence over time was produced.

Calculation of IC_{50} values. The cell confluence (in %) was exported to Microsoft Excel (Microsoft Corporation, Redmond, WA, USA) to calculate the inhibition of the cell growth. The last time point from the measurement of each

© 2019 The Authors. *Journal of Pharmacy and Pharmacology* published by John Wiley & Sons Ltd on behalf Royal Pharmaceutical Society, **72** (2020), pp. 236–248

concentration was taken as the maximal confluence was then reached. The calculation was done as described in equation 1.

$$\text{inhibition}(\%) = 100 * \left(1 - \frac{\text{confluence (under treatment)}[\%]}{\text{confluence(without treatment)}[\%]}\right) \quad (1)$$

The inhibition value was then transferred to Origin 2018b (OriginLab, Northampton, MA, USA) to generate a graph showing the inhibition in dependence of the common logarithm of the concentration. First, a scatter diagram was generated. The fitting of the curve was done by non-linear, sigmoidal, dose/response regression. The non-linear regression was calculated with equation 2.

$$y = \text{A1} + \frac{\text{A2} - \text{A1}}{1 + 10^{(\log_{x_0} - x) * p}} \quad (2)$$

with y being the inhibition in %, A1 being the horizontal approach to the lowest value in inhibition (bottom (left) asymptote), A2 being the horizontal approach to the highest value in inhibition (top (right) asymptote), A1 < A2, $\log_{x0}$ being the centre of the curve, x being the common logarithm of the concentration and p being the hill slope. At an inhibition of 50%, the x value is equivalent to the $\log_{10}(IC_{50})$ which then had to be transformed to the IC_{50} value. From the obtained values, the mean value and the corresponding standard deviation (SD) were calculated.

Cytotoxicity assay. The A427 cells were grown on a sterile 96-well plate (TPP) at 37 °C until a confluence of approx. 90% was reached. The medium was then removed. Afterwards, the plate was blocked with 200 µl of medium containing 1% BSA and washed with 200 µl of medium. 150 µl of medium and 50 µl of the diluted test compounds were added to each well. As a positive control for a maximum cytotoxicity, 0.1% Triton X was used. The negative control was the medium without a test compound. This was incubated for 3 and 24 h at 37 °C. The final concentrations of the test compounds in the assay were 50 and 5 µM, respectively.

After the incubation, 25 µl of supernatant and 50 µl of LDH-assay reagent (1 U/ml diaphorase, 1% sodium lactate, 0.1% NAD^+, 0.08% BSA and 0.4% iodonitrotetrazolium chloride in 75 mM PBS) were transferred to a clear 96-well plate (Diagonal GmbH & Co. KG, Münster, Germany), previously blocked with BSA (see above). The plate was incubated at 37 °C for 45 min. After the incubation, the absorption was measured at a wavelength of 490 nm in the plate reader. The obtained results were then put into relation to the controls.

Results and Discussion

Receptor selectivity

σ_1 affinity and selectivity over σ_2 receptor

The σ affinities of **1**–**6** were determined in competition experiments with [^{3}H]-(+)-pentazocine and [^{3}H]DTG as radioligands.[42–44] Homogenates from guinea pig brain (σ_1) and rat liver (σ_2) were used as receptor material. All spirocyclic thienopyrans included in this study show a very high selectivity for the σ_1 receptor (Table 1). Only for the thienofuranone **3,** a moderate σ_2 affinity (K_i = 379 nM) was observed. The combination of the slightly lower σ_1 affinity (K_i = 16 nM) with moderate σ_2 affinity resulted in a reduced selectivity of this compound. The increased σ_2 affinity could be attributed to the unique carbonyl moiety serving as H-bond acceptor or the different structure of the furan ring together with the sp^2 hybridization in 3-position.

Selectivity over opioid and NMDA receptors

To elucidate the selectivity of the spirocyclic thiophenes **1**–**6**, a comprehensive screening of the compounds at opioid receptors and the NMDA receptor was performed. Although the σ_1 receptor is not structurally related to the NMDA receptor, many compounds binding to the GluN2B subunit of the NMDA receptor show high affinity to both σ receptor subtypes, including the lead compound ifenprodil.[30] Therefore, the NMDA receptor was included in this study. The affinities to the µ-, δ- and κ-opioid receptor subtypes (MOR, DOR, KOR) were determined with

Table 1 σ Receptor affinity and selectivity of spirocyclic thienopyrans, thienofuranone **3** and reference compounds (+)-pentazocine and haloperidol

Compd.	K_i ± SEM [nM][a,b]		σ_1/σ_2 selectivity
	σ_1	σ_2	
1[35]	0.22 ± 0.06	806	>1000
2[35]	0.25 ± 0.14	923	>1000
3[36]	16 ± 7	379	24
4[37]	1.9 ± 0.4	16%	>500
5[37]	16 ± 6	17%	>60
6[38]	0.32 ± 0.09	1260	>1000
(+)-pentazocine	5.4 ± 0.5	–[c]	
Haloperidol	6.6 ± 0.9	125 ± 33	19

[a]In case of high affinity (K_i < 100 nM), the experiments were performed as triplicate (n = 3) and SEM values are given. [b]Values in % reflect the inhibition of the radioligand binding at a test compound concentration of 1 µM. [c]Due to the addition of (+)-pentazocine in this assay, σ_2 affinity of (+)-pentazocine cannot be determined in this assay.

© 2019 The Authors. *Journal of Pharmacy and Pharmacology* published by John Wiley & Sons Ltd on behalf Royal Pharmaceutical Society,

homogenates from guinea pig (MOR and KOR) and rat brain (DOR). For the determination of affinity to the PCP binding site, a membrane preparation of pig brain cortex was used,[40,41] while membrane fragments from recombinant mouse fibroblasts stably expressing the GluN1a/GluN2B subunits of the NMDA receptor were used in the assay for the ifenprodil binding site of the GluN2B subunit.[39] In Table 2, the radioligands employed in each binding assay and affinity data for reference compounds for each assay are listed.

For all compounds, a very low affinity to MOR was observed. Surprisingly, a low-to-moderate affinity to the KOR and DOR was observed for the spirocyclic thiophenes **1**, **2** and **6**. The highest affinity was recorded for the thieno [3,4-c]pyran **1**, while the shift of the S atom to the other positions of the annulated thiophene ring caused a slight decrease of MOR and DOR affinity. The arylated spirocyclic thiophenes **2** and **5** and the lactone **3** show only negligible affinity to all opioid receptor subtypes.

The interaction of all investigated compounds with the PCP binding site of the NMDA receptor is also negligible. At a concentration of 1 μM of each test compound, only a small amount of the radioligand [^{3}H]MK-801 was displaced in the competition assay. A very interesting result was found for the spirocyclic compound **2** bearing the *p*-cyanophenyl residue in the 1′-position of the thiophene ring. While this compound does not show any interaction with the opioid receptors and the PCP binding site, an unexpected affinity (K_i = 91 nM) to the GluN2B binding site of the NMDA receptor was determined. In contrast, the structurally closely related arylated compound **5** did not display measurable affinity to the GluN2B binding site rendering **5** the compound with the highest selectivity for the σ_1 receptor in this series.

Selectivity over 5-HT$_{1A}$, α_{1A}, α_{2A} receptors and 5-HT transporter

In order to gain additional information regarding the selectivity over other pharmacological targets, a screening of the spirocyclic thiophenes **1**, **3**, **4** and **6** was performed. An affinity to 5-HT$_{1A}$ receptors, the serotonin transporter (SERT) and the human α_{1A} adrenergic receptor were not observed for any of the compounds. For the non-arylated thiophenes **1** and **4,** a low affinity to the human α_{2A} adrenergic receptor was observed. At a concentration of 1 μM in the binding assay, an inhibition of 52% and 46% was recorded, respectively, indicating IC_{50} values of approximately 1 μM.

In conclusion, high-affinity spirocyclic σ_1 ligands **1**–**6** show high selectivity for the σ_1 receptor over the investigated related receptor systems.

Inhibition of the biosynthesis of ergosterol and cholesterol

To analyse potential inhibitory effects on the ergosterol and cholesterol biosynthesis, the non-arylated spirocyclic thiophene derivatives **1**, **3**, **4** and **6** were studied in cellular assays.[11,48–50] In the ergosterol biosynthesis assay, three different fungi species (*Candida glabrata*, *Saccharomyces cerevisiae* and *Yarrowia lipolytica*) were incubated with the spirocyclic thiophenes. Cell lysis and extraction yielded a crude fraction of fungal sterols, which were transformed into the corresponding trimethylsilyl ethers and analysed by GLC/MS. In neither of the three species, inhibitory effects of the spirocyclic thiophenes on the post-squalene part of ergosterol biosynthesis were found, including the fungal sterol $\Delta^{8/7}$-isomerase.

Table 2 Affinities of **1**–**6** and selected reference compounds to opioid and NMDA receptors

	K_i ± SEM [nM][a,b]				
Compd.	KOR [^{3}H]U-69,593	MOR [^{3}H]DAMGO	DOR [^{3}H]DPDPE	PCP [^{3}H]MK-801	GluN2B [^{3}H]ifenprodil
1	175	26%[b]	542	0%[b]	>1000
2	12%[b]	4%[b]	23%[b]	12%[b]	91 ± 42[a]
3	>1000	15%[b]	8%[b]	0%[b]	>1000
4	765	0%[b]	>1000	24%[b]	14%[b]
5	13%[b]	0%[b]	0%[b]	0%[b]	0%[b]
6	572	0%[b]	887	20%[b]	>1000
Naloxone	6.9 ± 0.5	2.1 ± 0.5	2.4 ± 0.5	–	–
Morphine	3.5 ± 6.0	3.9 ± 2.1	2.0 ± 0.3	–	–
MK-801	–	–	–	3.4 ± 0.8	–
Ifenprodil	–	–	–	–	10 ± 0.7

The tritiated radioligands used in the assays are mentioned, respectively. [a]In case of high affinity (K_i < 100 nM), the experiments were performed as triplicate (n = 3) and SEM values are given. [b]Values in % reflect the inhibition of the radioligand binding at a test compound concentration of 1 μM.

© 2019 The Authors. *Journal of Pharmacy and Pharmacology* published by John Wiley & Sons Ltd on behalf Royal Pharmaceutical Society,

In the cholesterol biosynthesis inhibition assay, human promyelocytic leukaemia cells (HL60) were incubated with the test compounds. Isolation and silylation of the sterol fraction were performed as described above, followed by GLC/MS analysis. For the thienopyrans **1**, **4** and **6,** analysis of the sterol pattern clearly indicated an inhibitory effect on the human sterol C14-reductase at high concentrations (50 μM), evident from an accumulation of the intermediate 4,4-dimethyl-5α-cholesta-8,14-dien-3β-ol in the biological samples. For the thienofuranone **3**, accumulation of zymostenol (cholest-8-en-3β-ol) clearly indicated an inhibition of the mammalian sterol $\Delta^{8/7}$-isomerase. These results were unexpected since the related human enzymes do not even show a structural similarity to the σ_1 receptor. Similar results were obtained by us before for aminomethyl-substituted spiroketals.[51] It is noteworthy that the inhibition of the mammalian sterol C14-reductase was detected for all three isomeric thienopyrans, regardless of the position of the S atom in the thiophene ring. However, since the sterol C14-reductase is located in the ER membranes, a modulatory effect of the σ_1 receptor acting as a chaperone might provide an explanation for the inhibitory effect of the spirocyclic σ_1 ligands on this enzyme.

Interaction with voltage-gated Ca^{2+} channels

With the aim to study the functional activity of the spirocyclic σ_1 ligands, one non-arylated (**1**) and one arylated compound (**2**) of the set were chosen to assess the influence on voltage dependent intracellular Ca^{2+} levels in retinal ganglion cells.[52] In short, the cells were preincubated with the Ca^{2+} sensitive fluorescent dye fura-2-AM and the test compound. Subsequently, the cells were depolarized with KCl to initiate influx of Ca^{2+} ions.

Both test compounds were not able to inhibit the KCl-induced Ca^{2+} influx, suggesting that they are not acting as σ_1 agonists. To study a possible antagonistic effect, the test compounds were co-incubated with the σ_1 agonist opipramol. The inhibitory effect of opipramol was reversed by the *p*-cyanophenyl substituted thiophene **2** in a dose-dependent manner (Figure 2). Therefore, **2** can be classified as an σ_1 antagonist in this assay system. For the non-arylated thiophene **1,** an increase of the KCl-induced Ca^{2+} influx was not observed.

Analgesic activity in the capsaicin assay

The analgesic activity of the spirocyclic thiophenes **1**, **4**, **5** and **6** was investigated in a capsaicin assay.[31] In this assay, mice were injected with 1 μg capsaicin in the right hind paw to induce hypersensitivity. After 15 min, a punctuate mechanical stimulation was applied with a nonflexible filament to the hind paw. When a paw withdrawal response of the animal occurred, the stimulation was automatically terminated and the response latency time recorded. The test compounds were injected intraperitoneally 5 min before the capsaicin treatment. For compounds **1**, **4** and **5,** a significant analgesic effect with a prolonged response latency time was observed (Figure 3). In addition to the pharmacological effect, the assay also demonstrates that the compounds are acting as σ_1 antagonists, which are in good accordance with the results of the retinal ganglion Ca^{2+} influx assay. For the thieno[3,2-c]pyran **6,** only weak analgesic activity was found. However, in contrast to the other test compounds **6** was administered 30 min before the capsaicin treatment so a metabolic degradation might explain the reduced activity.

Inhibition of ER stress in mouse pancreatic β-cells

The effect of the spirocyclic piperidine **1** on murine pancreatic β-cells was investigated by an apoptosis assay. Briefly, the cells were incubated with the test compound in standard medium before ER stress was induced by treatment with a high concentration of cyclopiazonic acid (CPA, 10 μM). CPA is an inhibitor of SERCA, a Ca^{2+} ATPase that transfers Ca^{2+} from the cytosol of the cell to the lumen of the ER. The Ca^{2+} depletion of the ER causes an increased rate of apoptosis. The apoptotic rate was determined by counting the number of total and apoptotic cells,

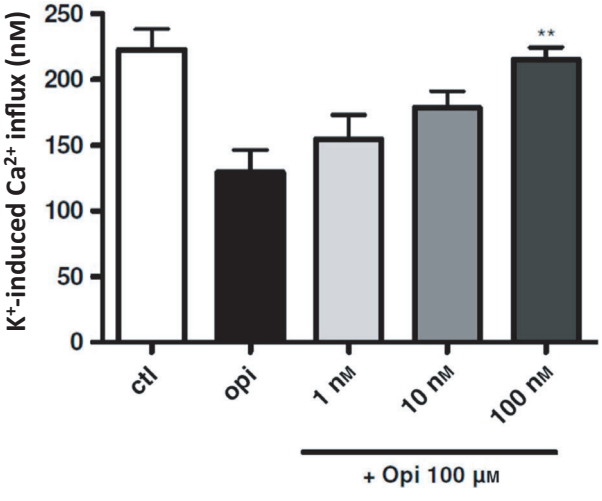

Figure 2 Reversal of the opipramol (Opi) induced inhibition of Ca^{2+} influx by the spirocyclic piperidine **2**. KCl-induced Ca^{2+} influx was measured by fura-2-AM imaging. Cells were preincubated for 30 min with fura-2-AM before stimulation with 20 mM KCl. Data were analysed by one-way ANOVA. Changes are mean ± SEM from three experiments (n = 3). Significance ** indicates $P < 0.01$.

© 2019 The Authors. *Journal of Pharmacy and Pharmacology* published by John Wiley & Sons Ltd on behalf Royal Pharmaceutical Society,

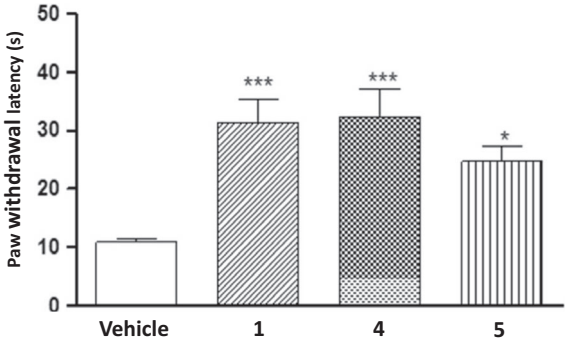

Figure 3 Effects of i.p. administration of **1**, **4** and **5** or vehicle (40 mg/kg) on mechanical hypersensitivity induced by intraplantar injection of capsaicin (1 μg) to mouse hind paw. The results represent the latency to hind paw withdrawal after stimulation with a filament at 0.5 g force. Bars and vertical lines represent the mean ± SEM from an independent group of animals (n = 7–13). *P < 0.05; ***P < 0.0001 (Newman–Keuls multiple comparison test post ANOVA).

respectively.[54] Islet cells were preincubated overnight with the σ_1 ligand before addition of CPA for another 24 h. Compound **1** slightly increased apoptotic cell death (TUNEL-positive cells, control: 0.16 ± 0.08%, + compound **1**, 1 μM: 1.8 ± 0.2%, n = 3 independent preparations, P < 0.05). An effect of the σ_1 antagonist **1** on the CPA-induced apoptosis was not observed (TUNEL-positive cells, CPA 10 μM: 3.6 ± 0.7%, + compound **1**, 1 μM: 3.02 ± 0.82%, n = 3, n.s.). Obviously, the test compound neither increased nor prevented the release of Ca^{2+} ions from the ER into the cytoplasm under stress conditions.

Inhibition of the growth of tumour cells

The influence of the σ_1 ligands on the proliferation of the tumour cell lines A427 (non-small-cell lung cancer), LCLC-103H (large cell lung cancer), 5637 (bladder cancer) and DAN-G (pancreatic cancer) was determined *in vitro* by a crystal violet staining assay. (+)-Pentazocine and haloperidol were included as reference compounds. The results are summarized in Table 3.

The cytotoxic effects of thienopyrans **1**, **2** and **5** on the non-small-cell lung cancer line A427 and the bladder cancer cell line 5637 are highly remarkable. These compounds inhibit the proliferation of both cell lines with IC_{50} values in the range between 2.6 and 9.1 μM. In the case of A427 cells, the same effect was observed for the σ_1 antagonist haloperidol, while the σ_1 agonist (+)-pentazocine did not show growth inhibiting effects. This observation is very interesting as the thienopyrans **1**, **2** and **5** have also been classified as antagonists in the functional assays described above. Similar results have been reported for other classes of σ ligands on this cell line.

For the 5637 cell line, it should be noted that cytotoxic effects were found for both (+)-pentazocine and haloperidol which indicates that the antiproliferative activity might not be related to the σ_1 receptor in this case.

A cytotoxic activity of lactone **3** and thieno[2,3-c]pyran **4** was abundant on all investigated cell lines. At least for **4,** this observation was surprising as not only the chemical structure but also the binding data and functional activity are very similar to the thieno[3,4-c]pyran **1**.

The thienopyran **2** bearing a *p*-cyanophenyl moiety shows a rather unselective inhibition of tumour cell growth with very similar IC_{50} values over all cell lines, indicating rather unspecific cytotoxicity than a σ receptor-mediated effect.

Analysis of the effects of spirocyclic thiophenes 2 and 5 on proliferation and morphology of the human tumour cell line A427

In the screening of different human tumour cell lines, the spirocyclic thiophenes **2** and **5** showed strong inhibition of the proliferation of the A427 tumour cell line. Therefore, these compounds were selected to determine the effects on this cell line in more detail. The A427 cells were incubated in the Live Cell Imager IncuCyte® S3, which allows permanent observation of the morphology and behaviour of cells over a long period without interruption of the incubation process. Both spirocyclic compounds led to inhibition of the proliferation of the A427 cell line. The cyanophenyl substituted thiophene **2** possessing higher σ_1 affinity revealed 3-fold stronger inhibition of cell proliferation than the phenyl substituted spirocyclic thiophene **5** (Table 4). These data obtained by determination of the confluence in the live cell imager correlate well with those from the crystal violet staining assay shown in Table 3.

Table 3 Growth inhibition of human tumour cells

	IC_{50} ± SD (μM)			
Compd.	A427	LCLC-103H	5637	DAN-G
1	6.7 ± 1.8	>10	5.4 ± 3.8	>20
2	2.6 ± 1.7	3.5 ± 2.5	5.5 ± 2.9	2.9 ± 1.8
3	>10	>10	>10	>10
4	>10	>10	>10	>10
5	5.9 ± 3.6	>10	9.1 ± 6.0	>10
(+)-pentazocine	>20	>10	3.5 ± 0.9	>20
Haloperidol	9.6 ± 3.7	10.9 ± 1.9	2.3 ± 1.4	>20

Average 50% growth inhibition concentrations (IC_{50}) of **1**–**5** together with the effects of the reference compounds (+)-pentazocine and haloperidol on different tumour cell lines. The viability of the cells was determined after exposure to test compounds for 96 h. IC_{50} values with SD were performed in triplicate (n = 3).

© 2019 The Authors. *Journal of Pharmacy and Pharmacology* published by John Wiley & Sons Ltd on behalf Royal Pharmaceutical Society, **72** (2020), pp. 236–248

Table 4 Inhibition of cell proliferation and cytotoxicity of spirocyclic thiophenes **2** and **5**

Compound	σ_1 affinity $K_i \pm$ SEM (nM)	Confluence $IC_{50} \pm$ SD (μM)	Confluence in the presence of (+)-pentazocine $IC_{50} \pm$ SD (μM)[a]	Cytotoxicity (%)[b]
2	0.25 ± 0.14	4.3 ± 0.8	6.1 ± 1.9	65
5	16 ± 6	13 ± 1	8.8 ± 2.7	28
Haloperidol	6.6 ± 0.9	16 ± 3	24 ± 2	No effect
(+)-Pentazocine	5.4 ± 0.5	No effect	–	6.4

[a](+)-Pentazocine was added in a concentration of 10 μM. [b]Mean of two experiments after 24 h of incubation at a concentration of 50 μM of the test compound. % values are related to untreated controls.

Whereas (+)-pentazocine, which is regarded as σ_1 agonist did not influence the proliferation of the A427 tumour cells, the σ_1 antagonist haloperidol showed considerable inhibition of proliferation (IC_{50} = 16 μM). (Table 4) Therefore, it was investigated whether the tumour cell proliferation inhibition of the spirocyclic thiophenes **2** and **5** could be antagonized by (+)-pentazocine (10 μM). The effect of the more potent cyanophenyl derivative **2** was reduced in the presence of (+)-pentazocine, but the effect of the less potent phenyl derivative **5** could not be inhibited.

In addition to recording IC_{50} values, the morphology of the A427 cells upon incubation under various conditions was observed and analysed (Figure 4). At first the A427 cells appear vital (Figure 4a), but 48 and 96 h after addition of compound **2** (10 μM), cells were detached from the surface and cell fragments could be observed (Figure 4b). This cytotoxic effect of **2** could be antagonized at least partially by addition of (+)-pentazocine. Several cells were still attached to the surface, and the amount of cell fragments was reduced (Figure 4c). At a concentration of 50 μM of the spirocyclic thiophene **2,** the rescue effect of (+)-pentazocine was lower (Figure 4d). The less potent phenyl substituted thiophene **5** shows qualitatively the same effects as the cyanophenyl substituted derivative **2**, but to a lesser extent.

In order to analyse the cytotoxic effect of the spirocyclic thiophenes **2** and **5,** the lactate dehydrogenase (LDH) assay was performed. Damage or destruction of cells leads to release of LDH, which can be measured by UV-spectroscopic determination of a coloured formazane dye. At a concentration of 50 μM, the cyanophenyl derivative **2** demonstrated strong cytotoxic activity (65%) in this assay, whereas the cytotoxicity of the phenyl substituted derivative **5** is considerably lower (28%). This result nicely correlates with the unspecific inhibition of cell growth of the four tumour cell lines presented in Table 3.

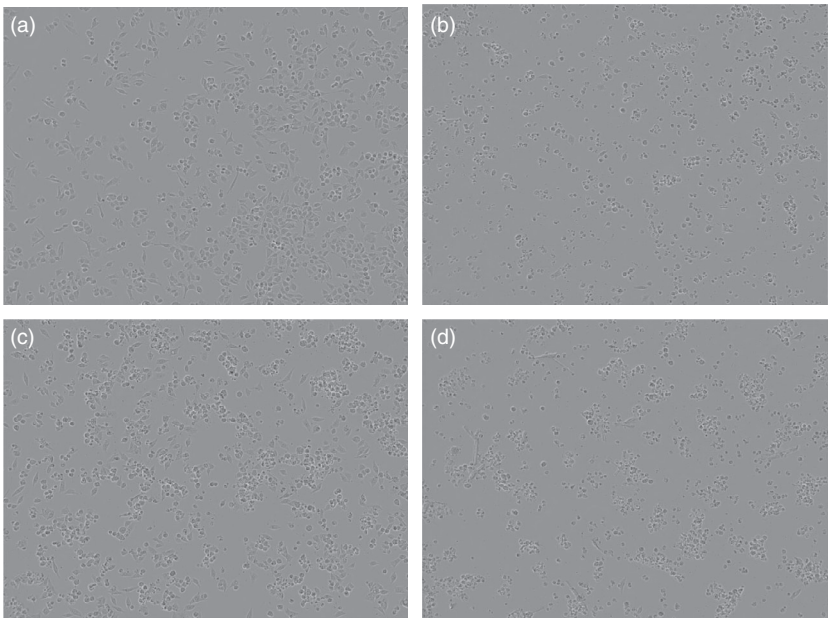

Figure 4 Morphology of A427 cells after treatment with various σ ligands. (a) Cell morphology directly before addition of compound **2**. (b) 96 h after treatment of the cells with compound **2** (10 μM). (c) 96 h after treatment of the cells with compound **2** (10 μM) and (+)-pentazocine (10 μM). (d) 96 h after treatment of the cells with compound **2** (50 μM) and (+)-pentazocine (10 μM).

© 2019 The Authors. *Journal of Pharmacy and Pharmacology* published by John Wiley & Sons Ltd on behalf Royal Pharmaceutical Society, **72** (2020), pp. 236–248

Conclusion

In this project, a comprehensive pharmacological study on a set of six spirocyclic arylated and non-arylated thiophenes, which had previously been identified as ligands of σ receptors, was performed. All compounds show high selectivity for the σ_1 receptor. The affinity to the σ_2 receptor and a variety of other pharmacological targets is very low or even negligible. Only for the thienopyran **2** bearing a *p*-cyanophenyl moiety, a moderate affinity to the ifenprodil binding site of GluN2B containing NMDA receptors was determined.

With an *in vivo* capsaicin assay, antiallodynic activity could be demonstrated for four compounds. This result proves not only the antagonistic activity of the compounds at the σ_1 receptor but also underlines the clinical potential of σ_1 ligands for the treatment of neuropathic pain.

An antiproliferative effect of the spirocyclic σ_1 ligands was observed, in particular for the non-small-cell lung cancer cell line A427. The IC_{50} values of **1, 2** and **5** are in the same range as observed for the σ_1 antagonist haloperidol, while the agonist (+)-pentazocine was not active. On the one hand, this result indicates a possible involvement of the σ_1 receptor in the physiology of this particular cell line; on the other hand, the correlation with haloperidol further confirms the postulated antagonistic activity of the ligands. However, an unspecific toxicity of the *p*-cyanophenyl substituted thienopyran **2** could not be ruled out. Observation of the morphology and behaviour of A427 tumour cells in the presence of **2** using a live cell imager demonstrated detachment of the cells and the formation of a large amount of cell fragments. This cytotoxic effect was confirmed in a LDH cytotoxicity assay. Antagonizing this cytotoxic effect by (+)-pentazocine confirms again the opposite effect as (+)-pentazocine, that is σ_1 antagonism.

An effect of σ_1 ligands on cell viability has also been seen in primary pancreatic β-cells. The classification based on the Ca^{2+} influx in the retinal ganglion cell provides a further approach to support the σ_1 antagonistic effect. An inhibition of the fungal sterol $\Delta^{8/7}$-isomerase was not observed for any of the compounds, despite the documented homology of σ_1 receptors and this enzyme. The inhibitory effect on the human sterol C14-reductase was unexpected but stimulates further research. Due to the localization of the sterol C14-reductase in the membrane of the ER, the activity of the enzyme might be regulated by the σ_1 receptor acting as a chaperone.

The very potent spirocyclic σ_1 receptor antagonist **1** slightly increased the apoptotic cell death of primary pancreatic β-cells. Due to the weak effects of the very potent σ_1 antagonist **1**, further experiments are required to show, whether the σ_1 receptor could be exploited as new promising target in diabetes research.

In summary, the comprehensive pharmacological profile of these high-affinity σ_1 receptor ligands provides further insight into the complex physiology of the enigmatic σ_1 receptor and interesting perspectives for the use of selective σ_1 receptor ligands as tools for pharmacological research and treatment.

Declarations

Conflict of interests

The Author(s) declare(s) no conflict of interest.

Acknowledgements

This work was performed within the framework of the International Research Training Group 'Complex Functional Systems in Chemistry: Design, Synthesis and Applications' in collaboration with the University of Nagoya. Financial support of this project by the IRTG Münster – Nagoya and the *Deutsche Forschungsgemeinschaft* is gratefully acknowledged.

Ethical committee approval of animal assay

Animal experiments were conducted following the rules of the local Committee of Animal Use and Care of our Institution (Animal Research Ethics Committee) and by Generalitat de Catalunya (Registry number: 9015-368574/2016) and international standards, including the Care and Use of Laboratory Animals Guidelines of the European Community (European Directive 2010/63/EU).

References

1. Martin WR *et al.* Effects of morphine-like and nalorphine-like drugs in non-dependent and morphine-dependent chronic spinal dog. *J Pharmacol Exp Ther* 1976; 197: 517–532.
2. Tam SW. Naloxone-inaccessible sigma-receptor in rat central nervous-system. *Proc Natl Acad Sci USA* 1983; 80: 6703–6707.
3. Vaupel DB. Naltrexone fails to antagonize the sigma-effects of Pcp and Skf 10,047 in the dog. *Eur J Pharmacol* 1983; 92: 269–274.
4. Quirion R *et al.* A proposal for the classification of sigma binding-sites. *Trends Pharmacol Sci* 1992; 13: 85–86.
5. Mash DC, Zabetian CP. Sigma receptors are associated with cortical limbic areas in the primate brain. *Synapse* 1992; 12: 195–205.

© 2019 The Authors. *Journal of Pharmacy and Pharmacology* published by John Wiley & Sons Ltd on behalf Royal Pharmaceutical Society, **72** (2020), pp. 236–248

6. Samovilova NN *et al.* (+)-[H-3]Skf 10,047 binding-sites in rat-liver. *Eur J Pharmacol* 1988; 147: 259–264.
7. Walker JM *et al.* Sigma-receptors – biology and function. *Pharmacol Rev* 1990; 42: 355–402.
8. Zabetian CP *et al.* [H-3]-(+)-Pentazocine binding to sigma-recognition sites in human 12rebellum. *Life Sci* 1994; 55: Pl389–Pl395.
9. Hanner M *et al.* Purification, molecular cloning, and expression of the mammalian sigma(1)-binding site. *Proc Natl Acad Sci USA* 1996; 93: 8072–8077.
10. Moebius FF *et al.* High affinity of sigma(1)-binding sites for sterol isomerization inhibitors: evidence for a pharmacological relationship with the yeast sterol C-8-C-7 isomerase. *Br J Pharmacol* 1997; 121: 1–6.
11. Müller C *et al.* Antifungal drug testing by combining minimal inhibitory concentration testing with target identification by gas chromatography-mass spectrometry. *Nat Protoc* 2017; 12: 947–963.
12. Aydar E *et al.* The sigma receptor as a ligand-regulated auxiliary potassium channel subunit. *Neuron* 2002; 34: 399–410.
13. Schmidt HR *et al.* Structural basis for sigma(1) receptor ligand recognition. *Nat Struct Mol Biol* 2018; 25: 981–987.
14. Schmidt HR *et al.* Crystal structure of the human sigma 1 receptor. *Nature* 2016; 532: 527–529.
15. Hellewell SB *et al.* Rat-liver and kidney contain high-densities of sigma (1) and sigma(2) receptors – characterization by ligand-binding and photoaffinity-labeling. *Eur J Pharmacol Mol Pharmacol Sect* 1994; 268: 9–18.
16. Fontanilla D *et al.* The hallucinogen N, N-Dimethyltryptamine (DMT) is an endogenous sigma-1 receptor regulator. *Science* 2009; 323: 934–937.
17. Monnet FP, Maurice T. The sigma(1) protein as a target for the non-genomic effects of neuro(active)steroids: molecular, physiological, and behavioral aspects. *J Pharmacol Sci* 2006; 100: 93–118.
18. Su TP *et al.* When the endogenous hallucinogenic trace amine N, N-dimethyltryptamine meets the sigma-1 receptor. *Sci Signal* 2009; 2: pe12.
19. Cobos EJ *et al.* Pharmacology and therapeutic potential of sigma(1) receptor ligands. *Curr Neuropharmacol* 2008; 6: 344–366.
20. Hashimoto K. Role of sigma-1 receptors in the treatment of social anxiety disorders. *Int J Neuropsychopharmacol* 2004; 7: S112.
21. Hayashi T, Su TP. sigma-1 receptor ligands – potential in the treatment of neuropsychiatric disorders. *CNS Drugs* 2004; 18: 269–284.
22. Maurice T, Su TP. The pharmacology of sigma-1 receptors. *Pharmacol Ther* 2009; 124: 195–206.
23. Vilner BJ *et al.* Sigma-1 and sigma-2 receptors are expressed in a wide variety of human and rodent tumor-cell lines. *Cancer Res* 1995; 55: 408–413.
24. Vilner BJ *et al.* Cytotoxic effects of sigma-ligands – sigma-receptor mediated alterations in cellular morphology and viability. *J Neurosci* 1995; 15: 117–134.
25. Meunier J, Hayashi T. Sigma-1 receptors regulate Bcl-2 expression by reactive oxygen species-dependent transcriptional regulation of nuclear factor kappa B. *J Pharmacol Exp Ther* 2010; 332: 388–397.
26. Rieusset J. Endoplasmic reticulum-mitochondria calcium signaling in hepatic metabolic diseases. *Biochim Biophys Acta Mol Cell Res* 2017; 1864: 865–876.
27. Thivolet C *et al.* Reduction of endoplasmic reticulum-mitochondria interactions in beta cells from patients with type 2 diabetes. *PLoS ONE* 2017; 12: e0182027.
28. Tubbs E, Rieusset J. Metabolic signaling functions of ER-mitochondria contact sites: role in metabolic diseases. *J Mol Endocrinol.* 2017; 58: R87–R106.
29. Hayashi T, Su TP. Intracellular dynamics of sigma-1 receptors (sigma (1) binding sites) in NG108-15 cells. *J Pharmacol Exp Ther* 2003; 306: 726–733.
30. Tchedre KT *et al.* Sigma-1 receptor regulation of voltage-gated calcium channels involves a direct interaction. *Invest Ophthalmol Vis Sci* 2008; 49: 4993–5002.
31. Entrena JM *et al.* Sigma-1 receptors are essential for capsaicin-induced mechanical hypersensitivity: studies with selective sigma-1 ligands and sigma-1 knockout mice. *Pain* 2009; 143: 252–261.
32. Gris G *et al.* Sigma-1 receptor and inflammatory pain. *Inflamm Res* 2015; 64: 377–381.
33. Sassonecorsi P *et al.* Ras-induced neuronal differentiation of Pc12 cells – possible involvement of Fos and Jun. *Mol Cell Biol* 1989; 9: 3174–3183.
34. Takebayashi M *et al.* A perspective on the new mechanism of antidepressants: neuritogenesis through sigma-1 receptors. *Pharmacopsychiatry* 2004; 37: S208–S213.
35. Meyer C *et al.* Exploitation of an additional hydrophobic pocket of sigma(1) receptors: late-stage diverse modifications of spirocyclic thiophenes by C-H bond functionalization. *Org Biomol Chem* 2011; 9: 8016–8029.
36. Meyer C *et al.* Late-stage C-H bond arylation of spirocyclic sigma(1) ligands for analysis of complementary sigma(1) receptor surface. *Eur J Org Chem* 2012; 30: 5972–5979.
37. Meyer C *et al.* Pd-catalyzed direct C-H bond functionalization of spirocyclic σ_1 ligands: generation of a pharmacophore model and analysis of the reverse binding mode by docking into a 3D homology model of the σ_1 receptor. *J Med Chem* 2012; 55: 8047–8065.
38. Oberdorf C *et al.* Thiophene bioisosteres of spirocyclic sigma receptor ligands: relationships between substitution pattern and sigma receptor affinity. *J Med Chem* 2012; 55: 5350–5360.
39. Schepmann D *et al.* Development of a selective competitive receptor binding assay for the determination of the affinity to NR2B containing NMDA receptors. *J Pharm Biomed Anal* 2010; 53: 603–608.
40. Banerjee A *et al.* Synthesis and SAR studies of chiral non-racemic

© 2019 The Authors. *Journal of Pharmacy and Pharmacology* published by John Wiley & Sons Ltd on behalf Royal Pharmaceutical Society,

dexoxadrol analogues as uncompetitive NMDA receptor antagonists. *Bioorg Med Chem* 2010; 18: 7855–7867.
41. Köhler J *et al*. Enantiomerically pure 1,3-dioxanes as highly selective NMDA and sigma(1) receptor ligands. *J Med Chem* 2012; 55: 8953–8957.
42. Hasebein P *et al*. Synthesis and pharmacological evaluation of like-and unlike-configured tetrahydro-2-benzazepines with the alpha-substituted benzyl moiety in the 5-position. *Org Biomol Chem* 2014; 12: 5407–5426.
43. Meyer C *et al*. Improvement of sigma (1) receptor affinity by late-stage C-H-bond arylation of spirocyclic lactones. *Bioorg Med Chem* 2013; 21: 1844–1856.
44. Miyata K *et al*. Synthesis and sigma receptor affinity of regioisomeric spirocyclic furopyridines. *Eur J Med Chem* 2014; 83: 709–716.
45. Contreras PC *et al*. Ifenprodil and Sl-82.0715 potently inhibit binding of [H-3] (+)-3-Ppp to sigma-binding sites in rat-brain. *Neurosci Lett* 1990; 116: 190–193.
46. Tangherlini G *et al*. Development of novel quinoxaline-based kappa-opioid receptor agonists for the treatment of neuroinflammation. *J Med Chem* 2019; 62: 893–907.
47. Wittig C *et al*. Stereoselective synthesis of conformationally restricted KOR agonists based on the 2,5-diazabicyclo [2.2.2]octane scaffold. *Org Biomol Chem* 2017; 15: 6520–6540.
48. Giera M *et al*. Fast and easy in vitro screening assay for cholesterol biosynthesis inhibitors in the post-squalene pathway. *Steroids* 2007; 72: 633–642.
49. Müller C *et al*. A gas chromatography–mass spectrometry-based whole-cell screening assay for target identification in distal cholesterol biosynthesis. *Nat Protoc* 2019; 14: 2546–2570.
50. Müller C *et al*. A convenient cellular assay for the identification of the molecular target of ergosterol biosynthesis inhibitors and quantification of their effects on total ergosterol biosynthesis. *Steroids* 2013; 78: 483–493.
51. Krojer M *et al*. Steroidomimetic aminomethyl spiroacetals as novel inhibitors of the enzyme delta 8,7-sterol isomerase in cholesterol biosynthesis. *Arch Pharm* 2014; 347: 108–122.
52. Grynkiewicz G *et al*. A new generation of Ca-2+ indicators with greatly improved fluorescence properties. *J Biol Chem* 1985; 260: 3440–3450.
53. Bracht K *et al*. Correlations between the activities of 19 anti-tumor agents and the intracellular glutathione concentrations in a panel of 14 human cancer cell lines: comparisons with the National Cancer Institute data. *Anticancer Drugs* 2006; 17: 41–51.
54. Gier B *et al*. Suppression of K-ATP channel activity protects murine pancreatic beta cells against oxidative stress. *J Clin Invest* 2009; 119: 3246–3256.

Supporting Information

Additional Supporting Information may be found in the online version of this article:

Appendix S1. The Supplementary Material contains experimental details of the receptor binding studies, inhibition of ergosterol and cholesterol biosynthesis, pain behavioural studies and inhibition of human tumor cell proliferation.

© 2019 The Authors. *Journal of Pharmacy and Pharmacology* published by John Wiley & Sons Ltd on behalf Royal Pharmaceutical Society, **72** (2020), pp. 236–248